Post-buckling and Large-deflection analysis of a sandwich FG plate with FG porous core based on the Carrera's Unified Formulation

K. Foroutan[a,b,1], E. Carrera[a,2], A. Pagani[a,3], H. Ahmadi[b,4]

[a] *MUL[2] Group, Department of Mechanical and Aerospace Engineering, Politecnico di Torino, Torino, Italy*

[b] *Faculty of Mechanical Engineering, Shahrood University of Technology, Shahrood, Iran*

Abstract

In this study, the unified formulation of a full geometrically nonlinear refined plate theory in a total Lagrangian approach is developed to study the post-buckling and large-deflection analysis of sandwich functionally graded (FG) plate with FG porous (FGP) core. The plate has three layers so that the upper and lower layers are FG and the middle layer (core) is the FGP, which is considered with four cases in terms of the porosity core distribution. These four cases are: (I) symmetric porosity distribution (SPD) core, (II) non-symmetric stiff porosity distribution (NSTPD) core, (III) non-symmetric soft porosity distribution (NSOPD) core and (IV) uniform porosity distribution (UPD) core. The different two-dimensional (2D) plate structures kinematics are consistently implemented based on the Carrera's Unified Formulation (CUF) by means of an index notation and an arbitrary expansion function of the generalized variables in the thickness direction, leading to lower- to higher-order plate models with only pure displacement variables. Furthermore, a finite element approximation and the principle of virtual work are used to easily and straightforwardly formulate the nonlinear governing equations in a total Lagrangian manner, whereas a path-following Newton-Raphson linearization scheme based on the arc-length constraint is utilized to solve the full geometrically nonlinear problem. Numerical assessments consist of the response of large-deflection and post-buckling for square and slender sandwich FG plates with FG core under transverse uniform pressure and inplane compression loadings, respectively, are finally conducted to confirm the capabilities of the proposed CUF plate model to predict the post-buckling and large-deflection equilibrium curves with high accuracy.

Keywords: Carrera's Unified Formulation; Sandwich FG plate; FG porous core; Post-buckling; Large-deflection; Geometrical nonlinearity.

[*] Corresponding author.
E–mail addresses:
kamran.foroutan@polito.it (K. Foroutan), erasmo.carrera@polito.it (E. Carrera), alfonso.pagani@polito.it (A. Pagani), habibahmadif@shahroodut.ac.ir (H. Ahmadi)
[1] Ph.D.
[2] Professor of Engineering Mechanics.
[3] Assistant professor.
[4] Associate professor.

1. Introduction

The static and dynamic behavior of shells and plate in viewpoint of geometrically nonlinear is one of the important aspects of the analysis of such structure and very applicable in the various engineering applications and industries. So, several researchers have been focused on this field. So far some review articles are presented in the mentioned-field. For example, Kapania et al. [1] presented a review of the developments, for the researches related to before 1989, in the analysis of laminated beams and plates with an emphasis on shear effects and buckling. Also, in another paper, they [2] presented a summary of the developments for analysis of laminated beams and plates with an emphasis on vibrations and wave propagations behavior. In these studies, discussion of various shear-deformation theories, available theories the developed finite elements (FE), the buckling and post-buckling behavior of perfect and geometrically imperfect plates are described. The above-addressed papers have used analytical, numerical, and experimental approaches.

Also, Carrera [3] presented a study about a historical review of the theories that have been developed to analyze of multilayered structures by focusing on the Zig-Zag theories. Also, he described a piecewise continuous displacement field in the plate thickness direction. These studies have been concentrated on the plate and shell geometries, although, in some cases, beams are also considered. In this regard, Carrera and Kröplin [4] investigated the effects of Zigzag and interlaminar equilibria to examine large-deflection behavior and post-buckling analysis of multilayered composite plates, regarding the higher-order shear deformation theories (HSDT). The von Kármán theory in combined the recent mixed two-dimensional model, elsewhere denoted by the acronym Reissner-Mindlin zigzag continuity (RMZC) is utilized. Coda et al. investigated the effect of Zig-Zag in linear and nonlinear analysis of laminated plates and shells, without considering new degrees of freedom. In this paper, a new finite element formulation is presented combining Zig-Zag effect presence, regularization of transverse stresses, and cinematically exact description in the nonlinear geometric formulation of FEM [5]. Carrera and Parisch [6] evaluated the effects of geometrical nonlinear for thin and moderately thick multilayered composite shells using modified multilayered shear stiffnesses. These stiffnesses have been obtained via a variational method considering parabolic interlaminar continuous transverse shear stress fields and zig-zag form of the in-plane displacements along the thickness direction of shell.

Some studies have been investigated the nonlinear behavior of shells and plate utilizing the first-order shear deformation theory (FSDT) in conjunction with a type of nonlinear strain. Urthaler and Reddy [7] presented a mixed finite element model for the nonlinear bending analysis of laminated composite plates, regarding the FSDT of plates. A p-type Lagrangian basis is used to approximate the nodal degrees of freedom that consist of three displacements, two rotations, and three-moment resultants. The geometric nonlinearity in the sense of the von Kármán is included in the plate theory. Also, many researches have been used the higher-order shear deformation theory (HSDT) in conjunction with a type of nonlinear strain. In this regard, Reddy [8] presented an HSDT for plates, considering the von Kármán strains. This theory contains the same dependent unknowns as in the Hencky-Mindlin type FSDT and accounts for the parabolic distribution of the transverse shear strains through the thickness of the plate. They proved that, the suggested theory predicts the deflections, stresses, and frequencies more accurately in comparison with the FSDT and the classical plate theory.

According to Reissner-Mindlin’s theory in conjunction with a nonlinear theory for strain, the governing equation of motion is derived for large deformation prediction. Reddy and Chao [9] addressed nonlinear bending of laminated composite thick rectangular plates, using shear deformable theory accounting for the transverse shear and large rotations, regarding the Reissner-Mindlin's thick plate theory, the von Kármán theory, respectively. Azizian and Dawe [10] presented a general finite strip method analysis for isotropic rectangular plates considering the nonlinear geometric. To consider the effects of transverse shear deformation, the Mindlin plate theory is utilized. In numerical applications, a particular type of finite strip is used in which all five reference quantities (three displacements and two rotations) are represented by cubic polynomial interpolation across the strip whilst the ends of the strip are simply supported for bending/shearing behavior and immovable for membrane behavior. Turvey and Osman [11] derived the governing equations of isotropic rectangular Mindlin plates considering the large deflection behavior. The numerical solution is performed based on the DR algorithm, using interlacing and non-interlacing finite-differences. Carrera and Villani [12] analyzed nonlinear large deflections and stability FEM analysis of shear deformable compressed anisotropic multilayered flat panels, in the static elastic conservative cases. According to Reissner-Mindlin’s theory in conjunction with von Kármán nonlinearity, the suggested finite element model is developed.

Utilizing the analytical approach, Shukla and Nath [13] presented the solutions of nonlinear moderately thick laminated rectangular plates, undergoing moderately large deformations. The discretization of equations is performed using fast-converging Chebyshev polynomials.

Chia [14] investigated analytically the nonlinear bending with large deflection of an unsymmetrically laminated angle-ply rectangular plate subjected to lateral load. The nonlinear von Kármán-type is used in the formulation of governing equations. Alwar and Nath [15] used Chebyshev polynomials to analyze the circular plates, considering the large deflection effects. They depicted that the suggested method in the form of Chebyshev series has the property of rapid convergence and utilized this technique to analyze the post-buckling behavior of circular plates with initial curvature.

Utilizing the iterative finite difference technique Rushton [16] studied large deflexion of plates considering variable-thickness. Using the dynamic relaxation method, a general method is proposed for analyzing the deflexion of variable-thickness elastic plates. He included the nonlinear terms, because of the large deflexion of plates. Clarke and Gregory addressed incremental-iterative strategies for nonlinear analyses, regarding the geometric nonlinearity. The solution is based on a modified Newton-Raphson approach and a consistent mathematical is utilized for the iterative and load incrementation strategies [17].

By differential quadrature method and utilizing a Newton-Raphson approach, Striz et al. [18] analyzed the nonlinear bending behavior of thin isotropic circular plates, considering large deflections. Civalek investigated the static and dynamic analysis of thin rectangular plates resting on elastic foundation, regarding geometrically nonlinear. Considering von Kármán equations, governing equations of the plate are derived and discretized using the harmonic differential quadrature (HDQ) and finite differences (FD) methods [19].

A refined mixed shear flexible finite element for the geometrically linear and nonlinear analysis of laminated anisotropic plates is presented Putcha and Reddy [20]. The presented theory fulfilled the zero transverse shear stress boundary conditions. In the suggested method, the shear correction coefficients are not used. Librescu and Stein analyzed the post-buckling behavior of composite panels, considering geometrical imperfections, subjected to uniaxial/biaxial compressive loads. They developed a refined geometrically nonlinear theory for composite laminated plates [21]. Librescu and Chang addressed the static post-buckling of imperfect multilayered composite laminated double-curved shallow panels subjected to compressive edge loads. The effects of transverse normal stress, transverse shear deformation, the character of the in-plane boundary, and lamination conditions are considered [22]. Carrera and Villani [23] investigated the post-buckling of symmetrically compressed laminated thick plates to study the effects of boundary conditions. They examined the effects of transverse shear on the aeroelastic analysis of a composite rotor having antisymmetric configuration employing the finite element method.

For applying the finite element method to trace the nonlinear response, Tsai and Palazotto [24] presented a modified Riks approach, for the composite cylindrical shell, considering an HSDT. They used a Parabolic transverse shear in the thickness direction of the shell. Carrera [25] presented a study on arc-length-type methods, concerning the incremental strategies to solve the nonlinear set of algebraic equations deriving from the application of the finite element method. In this paper, two modified Risks-Wempner methods and a new algorithm to choose the appropriate root of a nonlinear constraint equation are proposed. Rivera et al. [26] presented a new 12-parameter shell finite element to analyze the large deformation of composite shell structures. This model is developed utilizing third-order thickness stretch kinematics and a high-order spectral/hp approximations.

Considering full Lagrangian-type geometrical nonlinearity, Kim and Chaudhuri [27] investigated the large deformation behavior of thick laminated composite shells. The analysis is performed according to the hypothesis of layerwise linear displacement distribution in the thickness direction. Dash and Singh [28] utilizing Green-Lagrange formulation, studied the transverse bending of shear deformable laminated composite plates for the large rotations and transverse shear. The governing equations are derived employing the HSDT, considering all higher-order nonlinear terms of strain-displacement relationships. To develop the proposed nonlinear model, a C^0 isoparametric finite element suggested. Coda [29] analyzed the static and dynamic plates and shells utilizing the orthotropic laminated finite element, as geometrically nonlinear with continuous stress distribution along transverse direction are considered. The total Lagrangian is used for kinematic description which avoids the use of the finite rotation concept. Also, to avoid the membrane locking, the finite element model as curved triangular by cubic approximation is applied. Alijani and Amabili [30] using Green-Lagrange for strain-displacement relationships, regarding all nonlinear terms, analyzed the nonlinear static bending and forced vibrations of rectangular plates. They considered rotary inertia, thickness deformation parameters, and third-order shear deformation to describe the shell kinematics. Alijani and Amabili [31], considering the thickness deformation effect, investigated the nonlinear forced vibrations of moderately thick functionally graded (FG) rectangular plates, regarding the HSDT. They selected all nonlinear terms in the in-plane and transverse displacements to consider the geometrically nonlinear strain-displacement.

Utilizing the Carrera Unified Formulation (CUF), Wu et al. [32] investigated the effectiveness of different geometrically nonlinear strain on the post-buckling and nonlinear behavior of composite beams, considering large-deflection. They used a full geometrically nonlinear Lagrangian approach to analyze the beam behavior. Pagani and Carrera [33] presented a unified theory of beams utilizing the Carrera Unified Formulation (CUF) and a full geometrically nonlinear Lagrangian approach, for analyzing the effect of geometrical nonlinearities of beams. With only pure displacement variables, low- to higher-order beam models are implemented by using the Lagrange polynomial expansions of the unknowns on the cross-section. Pagani and Carrera [34] analyzed the post-buckling, considering the large-deflection, for laminated composite beams by employing CUF. The governing equations of low- to higher-order beam theories are expressed via an appropriate index notation for laminated beams. Also, layer-wise kinematics is applied utilizing Lagrange polynomial expansions of the primary mechanical variables. The virtual work principle and a finite element approximation are utilized to derive the governing equations in a full Lagrangian manner. According to CUF [35, 36], using appropriate expansions using the generalized variables, the structural theories could be transformed into unified generalized kinematics formulation. According to the intrinsic scalable nature of Carrera Unified formulation, the nonlinear governing equations and the related finite element arrays of the theory of 3D full geometrically nonlinear structural can be consistently expressed in terms of fundamental nuclei for different kinematics. These fundamental nuclei represent the basic building blocks, when opportunely expanded, allow for the straightforward generation of lower- and higher-order finite element models.

This paper is outlined as follows: Section 2 is devoted relations of material properties for the layer of the sandwich FG plate and porosity core distribution. The geometrical and constitutive expressions, Green-Lagrange nonlinear geometrical relations, CUF, and the related FE are reported in Section 3. Section 4 briefly reports the solution adopted in this work for the resolution of the geometrical nonlinear FE equations. Numerical examples are finally considered in Section 5 to demonstrate the effects of various edge support conditions, porosity core distribution, and loading ways on the geometrically nonlinear response, while some concluding remarks are presented in Section 6.

2. Sandwich FG plate with FGP core

The sandwich FG plate with a FGP core, regarding the system of coordinate (x, y, z), is illustrated in Fig. 1, which has three layers so that the upper and lower layers are FG and the core is the FGP. x and y are the two in-plane directions and z is the plate thickness coordinate. The thickness, length in the x-direction, and length in the y-direction of the plate are denoted by h, a, and b respectively. Also, the material distributions of the sandwich FG plate with a FGP core are shown in Fig. 2. The thickness of the lower, FGP, and upper layers of the plate are denoted by h_b, $h_m$and h_u, respectively.

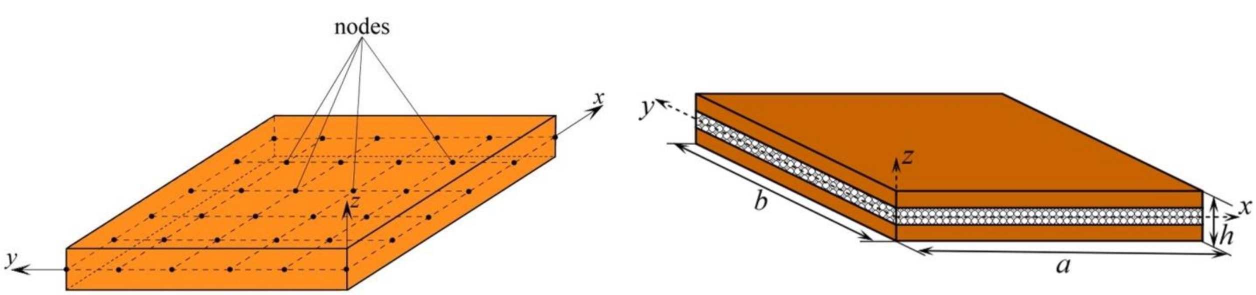

Fig. 1. Configuration of a sandwich FG plate with a FGP core utilizing 2D model.

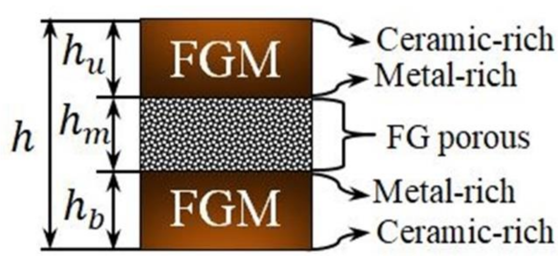

Fig. 2. The material distribution of sandwich FG plate with a FGP core.

The volume fractions regarding the power law can be written in the following form [37-40]:

$$V_c(z) = \left(\frac{2z + h}{2H}\right)^k \quad ; \quad H = h_u, h_b$$
$$V_m(z) = 1 - V_c(z) \tag{1}$$

In Eq. (1), $k \geq 0$ is the material power law index of the upper and lower FG layers of plate. The subscripts c and m refer to the ceramic and metal.

In the present article, four types of sandwich FG plate with a FGP core are examined which are demonstrated in Fig. 3. The Young's modulus of the sandwich FG plate with a FGP core is as follows [41-49]:

Type1: Sandwich FG plate with a SPD core

$$E(z) = \begin{cases} E_c + E_{mc}\left(\frac{2z + h - 2h_u}{2h_m}\right)^k & -\frac{h}{2} \leq z \leq -\frac{h}{2} + h_u \\ E_{\max}\left[1 - N_0 \cos\left(\frac{\pi z}{h_m}\right)\right] & -\frac{h}{2} + h_u \leq z \leq \frac{h}{2} - h_b \\ E_m + E_{cm}\left(\frac{2z + h - 2h_u}{2h_m}\right)^k & \frac{h}{2} - h_b \leq z \leq \frac{h}{2} \end{cases} \tag{2.a}$$

Type2: Sandwich FG plate with a NSTPD core

$$E(z) = \begin{cases} E_c + E_{mc}\left(\frac{2z + h - 2h_u}{2h_m}\right)^k & -\frac{h}{2} \leq z \leq -\frac{h}{2} + h_u \\ E_{\max}\left[1 - N_0 \cos\left(\frac{\pi z}{2h_m} + \frac{\pi}{4}\right)\right] & -\frac{h}{2} + h_u \leq z \leq \frac{h}{2} - h_b \\ E_m + E_{cm}\left(\frac{2z + h - 2h_u}{2h_m}\right)^k & \frac{h}{2} - h_b \leq z \leq \frac{h}{2} \end{cases} \tag{2.b}$$

Type3: Sandwich FG plate with a NSOPD core

$$E(z) = \begin{cases} E_c + E_{mc}\left(\frac{2z + h - 2h_u}{2h_m}\right)^k & -\frac{h}{2} \leq z \leq -\frac{h}{2} + h_u \\ E_{\max}\left[1 - N_0 \sin\left(\frac{\pi z}{2h_m} + \frac{\pi}{4}\right)\right] & -\frac{h}{2} + h_u \leq z \leq \frac{h}{2} - h_b \\ E_m + E_{cm}\left(\frac{2z + h - 2h_u}{2h_m}\right)^k & \frac{h}{2} - h_b \leq z \leq \frac{h}{2} \end{cases} \tag{2.c}$$

Type4: Sandwich FG plate with a UPD core

$$E(z) = \begin{cases} E_c + E_{mc}\left(\frac{2z + h - 2h_u}{2h_m}\right)^k & -\frac{h}{2} \leq z \leq -\frac{h}{2} + h_u \\ E_{\max}[1 - N_0\lambda] & -\frac{h}{2} + h_u \leq z \leq \frac{h}{2} - h_b \\ E_m + E_{cm}\left(\frac{2z + h - 2h_u}{2h_m}\right)^k & \frac{h}{2} - h_b \leq z \leq \frac{h}{2} \end{cases} \tag{2.d}$$

where

$$E_{mc} = E_m - E_c \tag{3}$$

$E(z)$ is Young's modulus, and N_0 is the coefficient of porosity for the Sandwich FG plate with a FGP core which are as follows:

$$N_0 = 1 - \frac{E_{\min}}{E_{\max}}; \quad 0 < N_0 < 1 \tag{4}$$

Also, λ in Eq. (2.d) for type 4 is given by:

$$\lambda = \frac{1}{N_0} - \frac{1}{N_0}\left(1 - \frac{2N_m}{\pi}\right)^2 \tag{5}$$

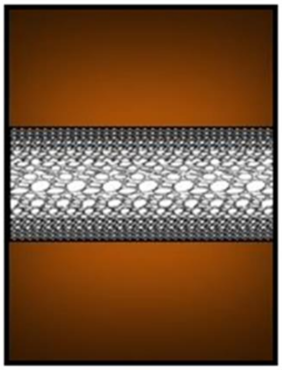

(a) Type1: Sandwich FG plate with a SPD core

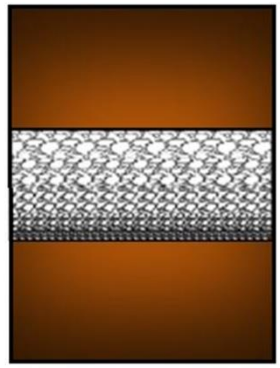

(b) Type2: Sandwich FG plate with a NSTPD core

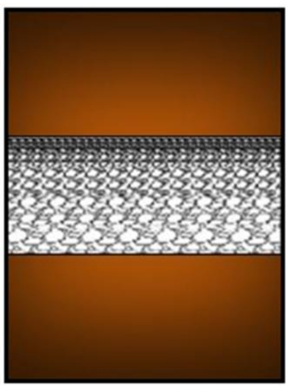

(c) Type3: Sandwich FG plate with a NSOPD core

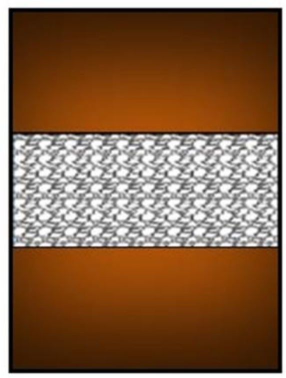

(d) Type4: Sandwich FG plate with a UPD core

Fig. 3. Cross-section of Sandwich FG plate with various porosity distributions core.

3. Formulation

3.1. Constitutive and geometrical relations

According to Fig. 1, the 3D displacement transposed vector ($\mathbf{u}$) is in the following form:

$$\mathbf{u}(x, y, z) = \{u_x \quad u_y \quad u_z\}^{\mathrm{T}} \tag{7}$$

The constitutive relations of stress-strain for materials with monoclinic symmetry are in the following form:

$$\sigma = \mathrm{C}\varepsilon \tag{8}$$

where the stress (σ), and strain (ε) vector are expressed as follows:

$$\sigma = \{\sigma_{xx}\ \sigma_{yy}\ \sigma_{zz}\ \sigma_{xz}\ \sigma_{yz}\ \sigma_{xy}\}^{\mathrm{T}},\ \ \varepsilon = \{\varepsilon_{xx}\ \varepsilon_{yy}\ \varepsilon_{zz}\ \varepsilon_{xz}\ \varepsilon_{yz}\ \varepsilon_{xy}\}^{\mathrm{T}} \tag{9}$$

The elastic matrix of material (C), is expressed as:

$$\mathrm{C} = \begin{bmatrix} C_{11} & C_{12} & C_{13} & 0 & 0 & C_{16} \\ C_{12} & C_{22} & C_{23} & 0 & 0 & C_{26} \\ C_{13} & C_{23} & C_{33} & 0 & 0 & C_{36} \\ 0 & 0 & 0 & C_{44} & C_{45} & 0 \\ 0 & 0 & 0 & C_{45} & C_{55} & 0 \\ C_{16} & C_{26} & C_{36} & 0 & 0 & C_{66} \end{bmatrix} \tag{10}$$

where C_{ij} are as follows:

$$\begin{aligned} &C_{16} = C_{26} = C_{36} = C_{45} = 0 \\ &C_{11} = C_{22} = C_{33} = \frac{(1-\upsilon)E(z)}{(1+\nu)(1-2\upsilon)} \\ &C_{12} = C_{13} = C_{23} = \frac{\nu E(z)}{(1+\nu)(1-2\upsilon)} \\ &C_{44} = C_{55} = C_{66} = \frac{E(z)}{2(1+\nu)} \end{aligned} \tag{11}$$

According to geometrical relations, the Green-Lagrange strain components are considered. So, the strain-displacement relations can be written as:

$$\varepsilon = \varepsilon_l + \varepsilon_{nl} = (\mathrm{b}_l + \mathrm{b}_{nl})\mathbf{u} \tag{12}$$

where b_l and b_{nl} are the linear and nonlinear operators, respectively, which are defined in the following form:

$$\mathrm{b}_l = \begin{bmatrix} \partial_x & 0 & 0 \\ 0 & \partial_y & 0 \\ 0 & 0 & \partial_z \\ \partial_z & 0 & \partial_x \\ 0 & \partial_z & \partial_y \\ \partial_y & \partial_x & 0 \end{bmatrix};\ \ \mathrm{b}_{nl} = \begin{bmatrix} \frac{1}{2}(\partial_x)^2 & \frac{1}{2}(\partial_x)^2 & \frac{1}{2}(\partial_x)^2 \\ \frac{1}{2}(\partial_y)^2 & \frac{1}{2}(\partial_y)^2 & \frac{1}{2}(\partial_y)^2 \\ \frac{1}{2}(\partial_z)^2 & \frac{1}{2}(\partial_z)^2 & \frac{1}{2}(\partial_z)^2 \\ \partial_x\partial_z & \partial_x\partial_z & \partial_x\partial_z \\ \partial_y\partial_z & \partial_y\partial_z & \partial_y\partial_z \\ \partial_x\partial_y & \partial_x\partial_y & \partial_x\partial_y \end{bmatrix} \tag{13}$$

where $\partial_x = \frac{\partial(\cdot)}{\partial x}$, $\partial_y = \frac{\partial(\cdot)}{\partial y}$ and $\partial_z = \frac{\partial(\cdot)}{\partial z}$.

3.2. Carrera unified formulation (CUF) and finite element (FE) approximation

The 3D displacement field $\mathbf{u}(x, y, z)$ according to the CUF for the 2D plate theory, can be expanded as a set of thickness functions depending only on the thickness coordinate z and the corresponding variables depending on the in-plane coordinates x and y. Specifically, we have:

$$\mathbf{u}(x, y, z) = F_s(z)\mathbf{u}_s(x, y);\ \ \ s = 0, 1, \ldots, N \tag{14}$$

where F_s are the functions of the coordinate z, $\mathbf{u}_s$ is the generalized displacement vector depending on the in-plane coordinates x and y, N denotes the order of expansion in the thickness direction, and the summing convention with the repeated index s is assumed. The choice of F_s determines the class of the 2D CUF plate model that is to be adopted.

The function $F_s(z)$, as Lagrange polynomials (LPs), will be considered along the z direction. Regarding this selection, the models based on Lagrange expansion (LE) CUF theories for plate are have been developed in the related literature [36]. In these suggested theories, i.e., LE models CUF, because the pure displacement component are utilized as the principal unknowns, therefore, the boundary conditions can be directley employed for these components of displacement. Also, by using layer-wise approach, which utilizes the LE model by default, for a multilayered composite plate, the conditions for interface consistency easily applied in the two consecutive layers. The details for LPs, which is not pertained directly to the CUF, is not refered here and are addressed by [50]. Brifely, the acronym LDN plate theories based on Layer-wise Displacement hypothesis are considered by means of an expansion with order N. In special cases, the functions for LE are employed as the linear with two-node (LD1), quadratic with three-node (LD2), and four-node cubic (LD3), in the z direction for formulating the kinematics, including the linear and higher order, according to CUF plate models .

For the sake of generality, the FEM is utilized to discretize the plate structure in the x-y plane. So, the generalized displacement vector $\mathbf{u}_s(x, y)$ is approximated as follows:

$$\mathbf{u}_s(x, y) = N_j(x, y)\mathbf{q}_{sj}; \quad j = 1, 2, \dots, p + 1 \tag{15}$$

where N_j is the jth shape function, p denotes the order of the shape functions and the repeated index j indicates summation. The vector of the FE nodal parameters $\mathbf{q}_{sj}$ is defined as:

$$\mathbf{q}_{sj} = \left\{ q_{x_{sj}} \quad q_{y_{sj}} \quad q_{z_{sj}} \right\}^{\mathrm{T}} \tag{16}$$

The specific expressions of the shape functions N_j are not illustrated here, and they can be found in Bathe [34, 50]. In the present study, the classical 2D four-node quadratic FE (Q4) will be adopted for the shape function in the x-y plane. It should be noted that the choice of the thickness expansion functions for various kinematics is completely independent of that of the plate FEs.

4. Nonlinear governing equations

The principle of virtual work is considered to evaluate the nonlinear FE governing equations. For a generic body, it reads:

$$\delta L_{\mathrm{int}} = \delta L_{\mathrm{ext}} \tag{17}$$

where δL_{int} and δL_{ext} is the virtual variation of the strain energy and the work of the external loads, respectively. It should be noted that the mathematical steps and equations illustrated hereafter are suitable for 2D models.

The left term of Eq. (17) is solved at first. Using the same notation shown in Eq. (9), it can be written as:

$$\delta L_{\text{int}} = \int_V \delta\varepsilon^T \sigma \mathrm{dV} \tag{18}$$

where V is the volume of the body. By substituting the constitutive (Eq. (8)) and geometrical relations (Eq. (14)) into Eq. (18), the virtual variation of the strain energy is obtained as follows:

$$\delta L_{\text{int}} = \delta \mathbf{q}_{sj}^T \left(\int_V \left(\mathbf{B}_l^{sj} + 2\mathbf{B}_{nl}^{sj} \right)^T \mathrm{C} \left(\mathbf{B}_l^{\tau i} + \mathbf{B}_{nl}^{\tau i} \right) \mathrm{dV} \right) \mathbf{q}_{\tau i} \tag{19}$$

The argument of the integral of the Eq. (19) represents the so-called secant stiffness matrix $\mathrm{K}_{\mathrm{S}}^{\mathrm{ij\tau s}}$, so that the equation can be written as:

$$\delta L_{\text{int}} = \delta \mathbf{q}_{sj}^T \mathrm{K}_{\mathrm{S}}^{\mathrm{ij\tau s}} \mathbf{q}_{\tau i} \tag{20}$$

The complete form of the secant stiffness matrix $\mathrm{K}_{\mathrm{S}}^{\mathrm{ij\tau s}}$ is omitted here for the sake of brevity, but can be found in [33, 51].

The right term of Eq. (17), omitting some mathematical steps, that can be found in Carrera et al. [35], can be written as:

$$\delta L_{\text{ext}} = \delta \mathbf{q}_{sj}^T \mathbf{P}_{sj} \tag{21}$$

so that Eq. (17) becomes:

$$\mathbf{K}_S^{ij\tau s} \mathbf{q}_{\tau i} - \mathbf{P}_{sj} = 0 \tag{22}$$

Eq. (22) can be arbitrarily expanded to reach any desired theory, from low- to higher-order ones, by choosing the values for $\tau, \mathrm{s} = 1, 2, \dots, \mathrm{M}$ and $\mathrm{i}, \mathrm{j} = 1, 2, \dots, \mathrm{p} + 1$, to give:

$$\mathbf{K}_S \mathbf{q} - \mathbf{P} = 0 \tag{23}$$

where $\mathbf{K}_S$, $\mathbf{q}$, and $\mathbf{P}$ are global, assembled FE arrays of the final structure.

To evaluate the geometrical nonlinear relations, the Eq. (23) needs to be solved. The process adopted in this work, is the same exhaustively shown in Pagani and Carrera [34], so interested readers are referred to it for a complete description. The main steps of the procedure are explained in the present study. The geometrical nonlinear problem is solved with the linearization of the Eq. (18) using the Newton-Raphson method, using Taylor's expansion around a known solution. What comes out from the linearization of the internal work is the so-called tangent stiffness matrix K_{T}, which complete form can be found in [33]. The resultant system of equations needs to be constrained. In the present study, an opportune arc-length path-following constraint is adopted. More detail about the arc-length method adopted can be found in Carrera [25] and Crisfield [52, 53].

5. Numerical results

Here, the capabilities of the appointed 3D full geometrically nonlinear CUF plate model to exactly predict the post-buckling and large-deflection equilibrium curves of sandwich FG plate with FG porous core, and also, the effects of various porosity distribution cores, FG material, and different loading states in a unified framework are illustrated. The thickness expansion functions are according to the Lagrange expansion (LE) CUF plate models. Also, for the FE, the four-node elements Q4 is used to approximate the displacement fields in the plate plane. In the following, at the first sub-section, the convergence and validation of the present approach are investigated and at the second sub-section, the effect of FG porosity on the large deflection response is illustrated that in the first section the large deflection response of square sandwich FG plate with FG porous core and the next section the large deflection and post-buckling response of slender sandwich FG plate with FG porous core is presented. Hereafter, the material parameters listed in Table 1, will be used for the extraction of the results.

Table 1 The material specifications of the sandwich FG plate with FG porous core

E_m(GPa) (Aluminum)	E_c(GPa) (Alumina)	N_0	k	ν
70	380	0.5	1	0.3

5.1. Convergence and validation of the present approach

Here, first, the large deflection of a square sandwich FG plate with FG porous core under a transverse uniform pressure P_z is considered. The CCCC edge condition used here is displayed in Fig. 4 along with the loading states. Also, the geometric parameters are listed in Table 2.

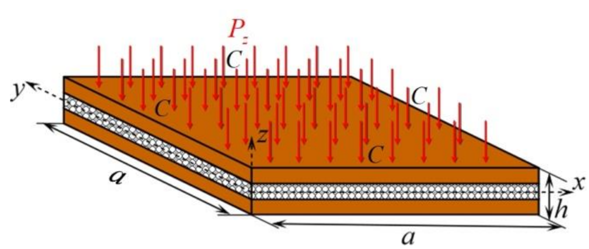

Fig. 4. Schematic of sandwich FG plate with FG porous core under the transverse uniform pressure with CCCC edge support conditions.

Table 2 The geometric specifications of the square sandwich FG plate with FG porous core

a(m)	b(m)	h_u(m)	h_m(m)	h_b(m)
1.2	1.2	0.025	0.072	0.025

First, the convergence analysis of this CUF plate element model will be performed through a regular mesh. Specifically, the large-deflection response of a square CCCC sandwich FG plate with a SPD core under uniform normal pressure P_z is illustrated in Fig. 5 for various in-plane mesh numbers (Fig. 5(a)) and LD2 and LD3 thickness expansion functions (Fig. 5(b)). As shown in Fig. 5(a), by increasing the number of the in-plane mesh, the fairly fast convergence rate is obtained. Furthermore, Fig. 5(b) illustrates that in order to accurately predict the equilibrium curves of large-deflection response, at least LD2 kinematics should be employed to reach an excellent convergence characteristic. So, the 8 × 8 in-plane mesh with one LD2 thickness expansion function will be considered, which as shown in Fig. 5, for the predicted large-deflection response to the pressure, can be assumed to have high accuracy.

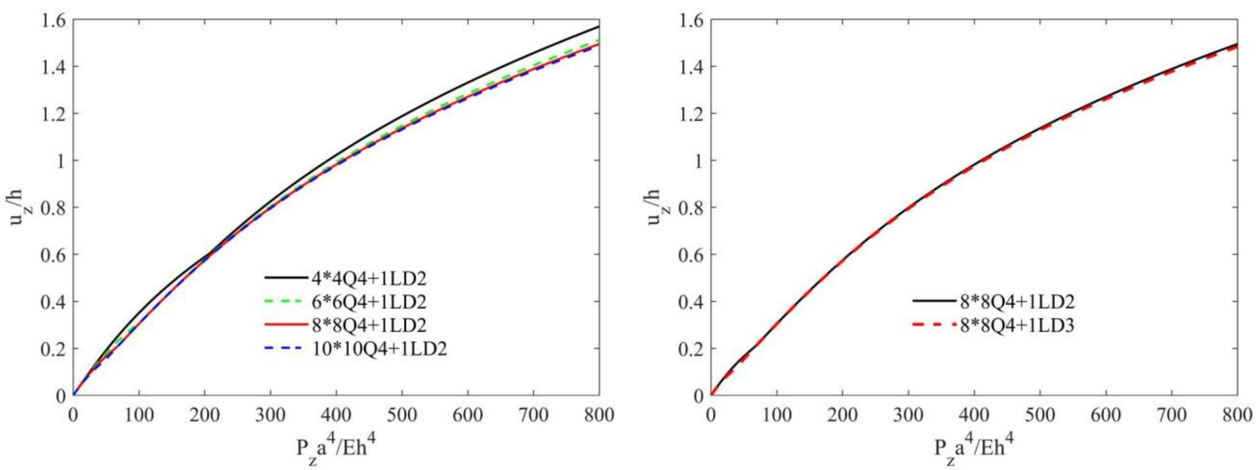

(a) Comparison of different in-plane mesh numbers

(b) Comparison of various orders of expansion functions in the thickness direction

Fig. 5. Convergence analysis of equilibrium curves for a square CCCC sandwich FG plate with a SPD core.

The large-deflection equilibrium curves of a CCCC functionally graded square plate under the uniform pressure are illustrated in Fig. 6 according to the 3D full geometrically nonlinear CUF plate model. In this figure, the effect of various material power-law indexes is studied. In order to validate the present work, $a/h = 5$, $E_c/E_m = 6$ is considered. It can be found in Fig. 6, for all the material power-law indexes, the nonlinear equilibrium curves according to the CUF plate model agree very well with those from Kim and Lee [54] in the entire pressure range for the functionally graded square plate. This excellent agreement manifests the validation of the CUF plate model and indicates that the von Kármán theory with first-order shear deformation modification can be effectively utilized to predict the large-deflection static response of the FG plates.

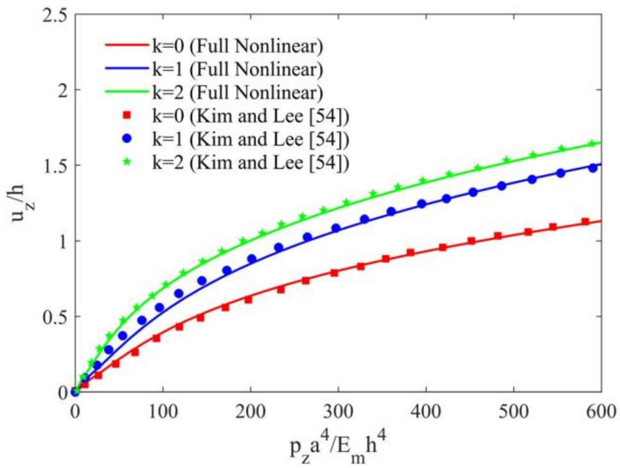

Fig. 6. Equilibrium curves of CCCC FG square plates under the transverse pressures.

5.2. The effect of FG porosity on the large deflection response

Here, the large-deflection and post-buckling analysis of sandwich FG plate with FG porous core subjected to uniform normal pressure and inplane compression loadings are investigated. In continue, first, the effect of porosity on the Large deflection response of square sandwich FG plate with FG porous core under to uniform normal pressure, and then the effect of porosity on the Large deflection and post-buckling response of slender sandwich FG plate with FG porous core under in-plane compression loadings are presented.

5.2.1. Large deflection response of square sandwich FG plate with FG porous core

The large-deflection equilibrium curves of a CCCC square sandwich FG plate with various porosity distributions core under the uniform pressure are illustrated in Fig. 7 according to the 3D full geometrically nonlinear CUF plate model. Regarding this figure, by increasing the value of pressure, the value of deflection is increased. As shown, the deflection of sandwich FG plate with SPD core is the most and the deflection of the sandwich FG plate with UPD core is the least.

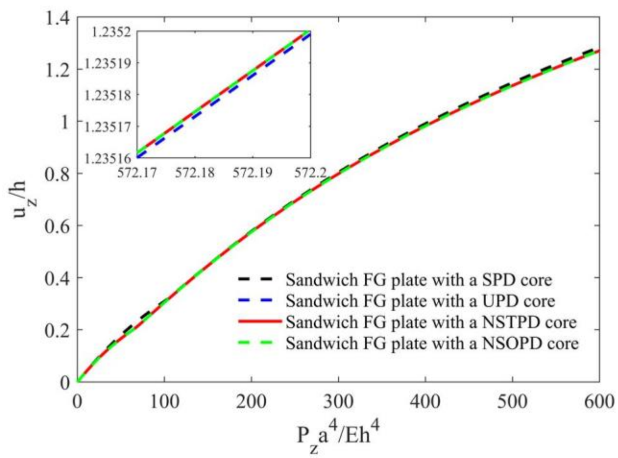

Fig. 7. Equilibrium curves of CCCC square sandwich FG plate with various porosity distributions core under the transverse pressures.

Fig. 8 shows the influence of porosity coefficients of the porous core on the geometrically nonlinear responses of the CCCC square sandwich FG plate with a SPD core under the transverse pressures. As shown, by increasing the porosity coefficients of the porous core, the value of deflection is decreased.

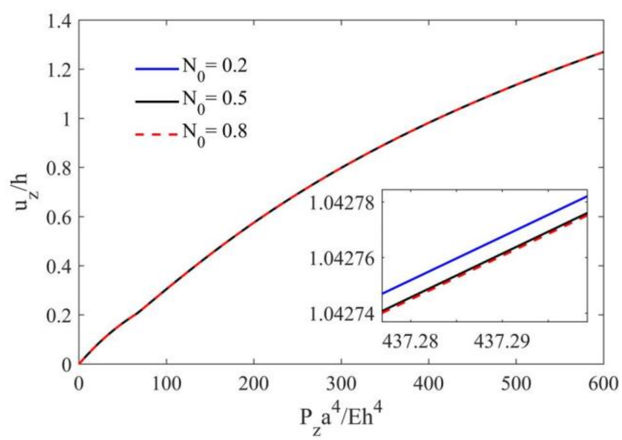

Fig. 8. Influence of porosity coefficients on the equilibrium curves of square sandwich FG plate with a SPD core subjected to transverse pressures.

5.2.2. Large deflection and postbuckling response of slender sandwich FG plate with FG porous core

In this sub-section, the enhanced abilities of the proposed 3D full geometrically nonlinear unified plate formulation to accurately predict the post-buckling equilibrium curves for slender sandwich FG plate with FG porous core subjected to in-plane compression loadings is demonstrated. The geometric parameters for this section are listed in Table 3. The large deflection response of the CCCC slender sandwich FG plate with FG porous core under the transverse uniform pressure P_z is shown in Fig. 5a, and, the slender sandwich FG plate with FG porous core under the line compression load P_x which is applied at the middle-line of the *y*-*z* cross-section at the two ends of the slender plate is illustrated in Fig. 5b. In this case, a uniform distribution of small transverse pressure D_p is applied to generate the post-buckling path. Specifically, the two movable simply-supported edge condition 'S_1' along the width (*y*-direction) satisfies $v = w = 0$ at $z = 0$ and $x = 0, a$, while another set of simply-supported opposite edges along the length (*x*-direction) satisfies $w = 0$ at $\mathrm{z} = 0$ and $y = 0, b$, which is represented by 'S_2'. In this section, the 10 × 5 in-plane mesh with one LD2 thickness expansion function is considered.

Table 3 The geometric specifications of the slender sandwich FG plate with FG porous core

a(m)	b(m)	h_u(m)	h_m(m)	h_b(m)
0.3	0.06	0.0012	0.0036	0.0012

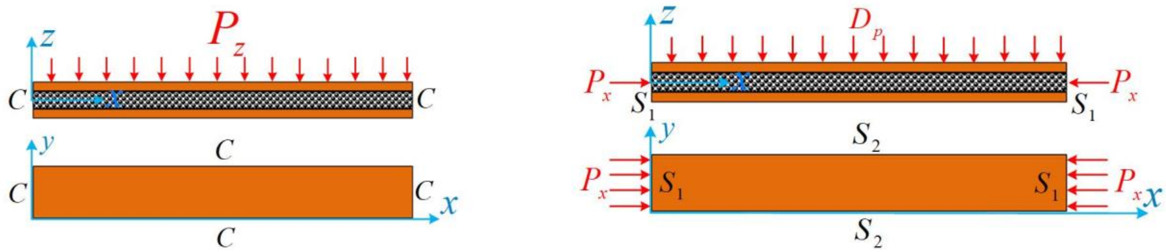

(a) sandwich FG plate with CCCC edge conditions (b) sandwich FG plate with $S_1S_2S_1S_2$ edge conditions

Fig. 9. Schematic diagram of the various edge support conditions under inplane compression loadings.

The post-buckling equilibrium curves of a CCCC slender sandwich FG plate with various porosity distributions core under the uniform pressure are shown in Fig. 10 according to the 3D full geometrically nonlinear CUF plate model. Regarding this figure, by increasing the value of pressure, the value of deflection is increased. As shown, the deflection of sandwich FG plate with UPD core is the least and the deflection of sandwich FG plate with other cores is the same and they are more than the deflection of sandwich FG plate with UPD core.

Fig. 11 illustrates the influence of porosity coefficients of the porous core on the post-buckling equilibrium curves of the CCCC slender sandwich FG plate with a SPD core under the transverse pressures. As shown, by increasing the porosity coefficients of the porous core, the value of pressure is decreased.

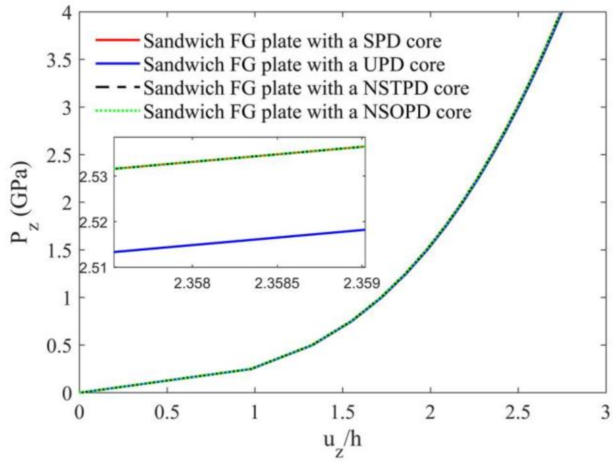

Fig. 10. Post-buckling equilibrium curves of CCCC slender sandwich FG plate with various porosity distributions core under the transverse pressures.

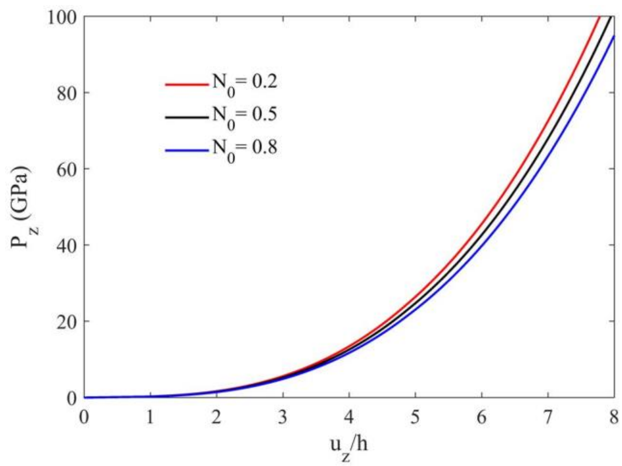

Fig. 11. Influence of porosity coefficients on the post-buckling equilibrium curves of slender sandwich FG plate with a SPD core subjected to transverse pressures.

The large-deflection equilibrium curves of a slender sandwich FG plate with various porosity distributions core subjected to the in-plane compression loadings are shown in Fig. 12 according to the 3D full geometrically nonlinear CUF plate model for $S_1S_2S_1S_2$ edge condition. Regarding this figure, by increasing the value of compression loadings, the value of deflection is increased. As shown, the deflection of sandwich FG plate with SPD core is the most and the deflection of sandwich FG plate with other cores is the same and they are more than the deflection of sandwich FG plate with UPD core. Also, it can be seen, for the low value of compression loadings, deflection has a downward jump, then by increasing the value of compression loadings, the value of deflection is increased.

Fig. 13 illustrates the influence of porosity coefficients of the porous core on the large-deflection equilibrium curves of the slender sandwich FG plate with a SPD core under the transverse pressures for $S_1S_2S_1S_2$ edge conditions. As shown, by increasing the porosity coefficients of the porous core, the value of deflection is increased.

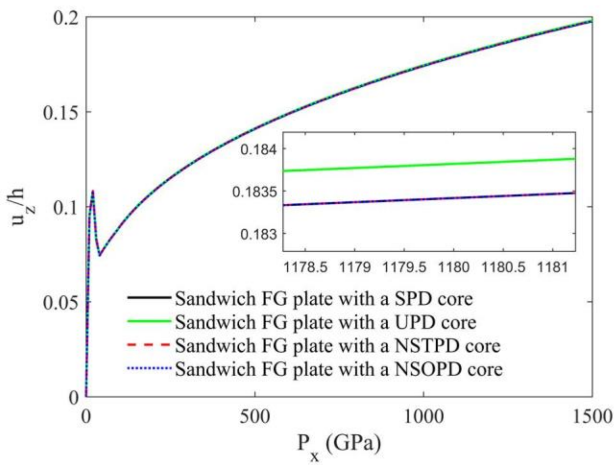

Fig. 12. Equilibrium curves of slender sandwich FG plate with various porosity distributions core under the in-plane compressive line loads.

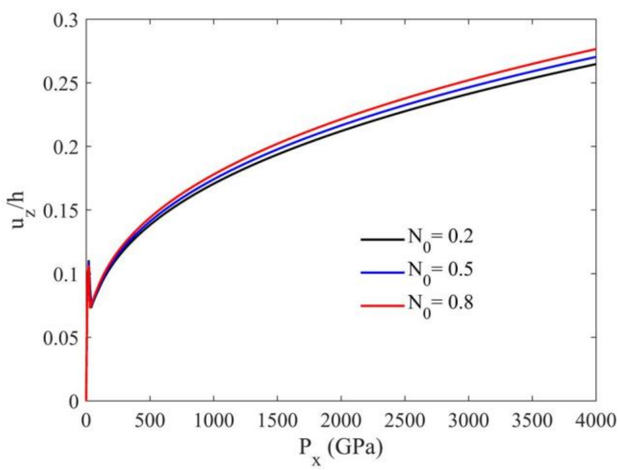

Fig. 13. Influence of porosity coefficients on the equilibrium curves of slender sandwich FG plate with a SPD core subjected to the in-plane compressive line loads.

6. Conclusions

In this work, the unified formulation of a full geometrically nonlinear refined plate theory in a total Lagrangian approach is developed to study the post-buckling and large-deflection analysis of sandwich functionally graded plate with FG porous core. The plate has three layers that the upper and lower layers are FG and the middle layer (core) is the FGP which is considered with four cases in terms of the porosity core distribution. In this study, the complete geometrically nonlinear, according the full Lagrangian-type formulation, according to the CUF plate theory are suggested. In a unified approach based on fundamental nuclei, the necessary descriptions of the secant and tangent stiffness matrices of the unified plate element have been constructed, regarding the CUF advantages. For solving the nonlinear algebraic relations, linearization method based on a Newton-Raphson approach is appliyed along with an arc-length constraint relationships, for several sample of isotropic rectangular plate numerically. To demonstrate the enhanced effectiveness and accuracy of the suggested CUF plate model for large-deflection, numerical evaluation is performed for the post-buckling response of square and slender sandwich functionally graded plate with FG porous core, which is exposed to transverse compressive and pressures loadings. In breifly, some principal conclusions are listed in the following:

- The enhanced effectiveness and accuracy of the suggested CUF plate models, exposed to transverse pressures for square plate, compared with the nonlinear geometric von Kármán relationships with the shear deformation modification, in the higher nonlinear area, yields more accurate results in the deflection of thick plate cases.
- For the square sandwich FG plate with various porosity distributions core subjected to the uniform pressure, the deflection of sandwich FG plate with SPD core is the most and the deflection of sandwich FG plate with UPD core is the least. Also, by increasing the porosity coefficients of the porous core, the value of deflection is decreased.
- For the slender sandwich FG plate with various porosity distributions core subjected to the uniform pressure or inplane compression loadings, the deflection of sandwich FG plate with UPD core is the least and the deflection of sandwich FG plate with other cores are the same and they are more than the deflection of sandwich FG plate with UPD core. Also, by increasing the porosity coefficients of the porous core, the value of pressure is decreased.

References

1. Kapania RK, Raciti S. Recent advances in analysis of laminated beams and plates. Part I-Sheareffects and buckling. *AIAA J* 1989; 27: 923-935.
2. Kapania RK, Raciti S. Recent advances in analysis of laminated beams and plates, part II: Vibrations and wave propagation. *AIAA J* 1989; 27: 935-946.
3. Carrera E. Historical review of zig-zag theories for multilayered plates and shells. *Appl Mech Rev* 2003; 56: 287-308.
4. Carrera E, Kröplin B. Zigzag and interlaminar equilibria effects in large-deflection and postbuckling analysis of multilayered plates. *Mech Compos Mater Struct* 1997; 4: 69-94.
5. Coda HB, Paccola RR, Carrazedo R. Zig-Zag effect without degrees of freedom in linear and non linear analysis of laminated plates and shells. *Compos Struct* 2017; 161: 32-50.
6. Carrera E, Parisch H. An evaluation of geometrical nonlinear effects of thin and moderately thick multilayered composite shells. *Compos Struct* 1997; 40: 11-24.
7. Urthaler Y, Reddy J. A mixed finite element for the nonlinear bending analysis of laminated composite plates based on FSDT. *Mech Adv Mater Struct* 2008; 15: 335-354.
8. Reddy J. A refined nonlinear theory of plates with transverse shear deformation. *Int J solids Struct* 1984; 20: 881-896.
9. Reddy J, Chao W. Non-linear bending of thick rectangular, laminated composite plates. *Int J Nonlin Mech* 1981; 16: 291-301.
10. Azizian Z, Dawe D. Geometrically nonlinear analysis of rectangular mindlin plates using the finite strip method. *Comput Struct* 1985; 21: 423-436.
11. Turvey G, Osman M. Elastic large deflection analysis of isotropic rectangular Mindlin plates. *Int J Mech Sci* 1990; 32: 315-328.

12. Carrera E, Villani M. Large deflections and stability FEM analysis of shear deformable compressed anisotropic flat panels. *Compos Struct* 1994; 29: 433-444.
13. Shukla K, Nath Y. Nonlinear analysis of moderately thick laminated rectangular plates. *J Eng Mech* 2000; 126: 831-838.
14. Chia CY. Large deflection of unsymmetric laminates with mixed boundary conditions. *Int J Nonlin Mech* 1985; 20: 273-282.
15. Alwar R, Nath Y. Application of Chebyshev polynomials to the nonlinear analysis of circular plates. *Int J Mech Sci* 1976; 18: 589-595.
16. Rushton K. Large deflexion of variable-thickness plates. *Int J Mech Sci* 1968; 10: 723-735.
17. Clarke MJ, Hancock GJ. A study of incremental-iterative strategies for non-linear analyses. *Int J Numer Methods Eng* 1990; 29: 1365-1391.
18. Striz AG, Jang SK, Bert CW. Nonlinear bending analysis of thin circular plates by differential quadrature. *Thin Wall Struct* 1988; 6: 51-62.
19. Civalek Ö. Harmonic differential quadrature-finite differences coupled approaches for geometrically nonlinear static and dynamic analysis of rectangular plates on elastic foundation. *J Sound Vib* 2006; 294: 966-980.
20. Putcha N, Reddy J. A refined mixed shear flexible finite element for the nonlinear analysis of laminated plates. *Comput Struct* 1986; 22: 529-538.
21. Librescu L, Stein M. Postbuckling of shear deformable composite flat panels taking into account geometrical imperfections. *AIAA J* 1992; 30: 1352-1360.
22. Librescu L, Chang MY. Imperfection sensitivity and postbuckling behavior of shear-deformable composite doubly-curved shallow panels. *Int J solids Struct* 1992; 29: 1065-1083.
23. Carrera E, Villani M. Effects of boundary conditions on postbuckling of compressed, symmetrically laminated thick plates. *AIAA J* 1995; 33: 1543-1546.
24. Tsai CT, Palazotto AN. A modified Riks approach to composite shell snapping using a high-order shear deformation theory. *Comput Struct* 1990; 35: 221-226.
25. Carrera E. A study on arc-length-type methods and their operation failures illustrated by a simple model. *Comput Struct* 1994; 50: 217-229.
26. Rivera MG, Reddy J, Amabili M. A new twelve-parameter spectral/hp shell finite element for large deformation analysis of composite shells. *Compos Struct* 2016; 151: 183-196.
27. Kim D, Chaudhuri RA. Full and von Karman geometrically nonlinear analyses of laminated cylindrical panels. *AIAA J* 1995; 33: 2173-2181.
28. Dash P, Singh B. Geometrically nonlinear bending analysis of laminated composite plate. *Commun Nonlin Sci Numer Simul* 2010; 15: 3170-3181.
29. Coda H. Continuous inter-laminar stresses for regular and inverse geometrically non linear dynamic and static analyses of laminated plates and shells. *Compos Struct* 2015; 132: 406-422.
30. Alijani F, Amabili M. Non-linear static bending and forced vibrations of rectangular plates retaining non-linearities in rotations and thickness deformation. *Int J Nonlin Mech* 2014; 67: 394-404.
31. Alijani F, Amabili M. Effect of thickness deformation on large-amplitude vibrations of functionally graded rectangular plates. *Compos Struct* 2014; 113: 89-107.
32. Wu B, Pagani A, Filippi M, Chen WQ, Carrera E. Accurate stress fields of post-buckled laminated composite beams accounting for various kinematics. *Int J Nonlin Mech* 2019. 111: 60-71.
33. Pagani A, Carrera E. Unified formulation of geometrically nonlinear refined beam theories. *Mech Adv Mater Struct* 2018; 25: 15-31.
34. Pagani A, Carrera E. Large-deflection and post-buckling analyses of laminated composite beams by Carrera Unified Formulation. *Compos Struct* 2017; 170: 40-52.
35. Carrera E, Giunta G, Petrolo M. *Beam structures: classical and advanced theories*. John Wiley & Sons, Chichester, UK, 2011.

36. Carrera E, Cinefra M, Petrolo M, Zappino, E. *Finite element analysis of structures through unified formulation*. John Wiley & Sons, Chichester, UK, 2014.
37. Osofero AI, Vo TP, Nguyen TK, Lee J. Analytical solution for vibration and buckling of functionally graded sandwich beams using various quasi-3D theories. *J Sandw Struct Mater* 2016; 18: 3-29.
38. Mekerbi M, Benyoucef S, Mahmoudi A, Tounsi A, Bousahla AA, Mahmoud SR. Thermodynamic behavior of functionally graded sandwich plates resting on different elastic foundation and with various boundary conditions. *J Sandw Struct Mater* 2019; 1099636219851281.
39. Tran TT, Nguyen NH, Do TV, Minh PV, Duc ND. Bending and thermal buckling of unsymmetric functionally graded sandwich beams in high-temperature environment based on a new third-order shear deformation theory. *J Sandw Struct Mater* 2019; 1099636219849268.
40. Wattanasakulpong N, Chaikittiratana A, Pornpeerakeat S. Vibration of size-dependent functionally graded sandwich microbeams with different boundary conditions based on the modified couple stress theory. *J Sandw Struct Mater* 2020; 22: 220-247.
41. Askari M, Saidi AR, Rezaei AS. An investigation over the effect of piezoelectricity and porosity distribution on natural frequencies of porous smart plates. *J Sandw Struct Mater* 2018; 1099636218791092.
42. Mojahedin A, Jabbari M, Khorshidvand AR, Eslami MR. Buckling analysis of functionally graded circular plates made of saturated porous materials based on higher order shear deformation theory. *Thin Wall Struct* 2016; 99: 83-90.
43. Jabbari M, Mojahedin A, Haghi M. Buckling analysis of thin circular FG plates made of saturated porous-soft ferromagnetic materials in transverse magnetic field. *Thin Wall Struct* 2014; 85: 50-56.
44. Wang Y, Wu D. Free vibration of functionally graded porous cylindrical shell using a sinusoidal shear deformation theory. *Aerosp Sci Technol* 2017; 66: 83-91.
45. Belica T. Malinowski M, Magnucki K. Dynamic stability of an isotropic metal foam cylindrical shell subjected to external pressure and axial compression. *J Appl Mech* 2011; 78: 041003.
46. Tu TM, Hoa LK, Hung DX, Hai LT. Nonlinear buckling and post-buckling analysis of imperfect porous plates under mechanical loads. *J Sandw Struct Mater* 2018; 1099636218789612.
47. Ga K, Gao W, Wu B, Wu D, Song C. Nonlinear primary resonance of functionally graded porous cylindrical shells using the method of multiple scales. *Thin Wall Struct* 2018; 125: 281-293.
48. Ahmadi H, Foroutan K. Nonlinear static and dynamic thermal buckling analysis of imperfect multilayer FG cylindrical shells with an FG porous core resting on nonlinear elastic foundation. *J Therm Stresses* 2020; 43: 629-649.
49. Foroutan K, Shaterzadeh AR, Ahmadi H. Nonlinear static and dynamic hygrothermal buckling analysis of imperfect functionally graded porous cylindrical shells. *Appl Math Model* 2020; 77: 539-553.
50. Bathe KJ. *Finite element procedures*. Prentice Hall, Upper Saddle River, NJ, 1996.
51. Carrera E, Pagani A, Augello R. Evaluation of geometrically nonlinear effects due to large cross-sectional deformations of compact and shell-like structures. *Mech Adv Mater Struct* 2018: 1-9.
52. Crisfield MA. A fast incremental/iterative solution procedure that handles “snap-through”. *Comput Struct* 1981; 16: 55-62.
53. Crisfield MA. An arc-length method including line searches and accelerations. *Int J Numer Methods Eng* 1983 19: 1269-1289.
54. Kim NI, Lee J. Geometrically nonlinear isogeometric analysis of functionally graded plates based on first-order shear deformation theory considering physical neutral surface. *Compos Struct* 2016; 153: 804-814.